Catalytic activities of mammalian epoxide hydrolases with *cis* and *trans* fatty acid epoxides relevant to skin barrier function

Haruto Yamanashi[1,2], William E. Boeglin[1], Christophe Morisseau[3], Robert W. Davis[4], Gary A. Sulikowski[4], Bruce D. Hammock[3], and Alan R. Brash[1]

From the Departments of Pharmacology[1] and Chemistry[4] and the Vanderbilt Institute of Chemical Biology, Vanderbilt University School of Medicine, Nashville, Tennessee 37232, the Department of Dermatology and Allergology, Juntendo University Graduate School of Medicine[2], 2-1-1 Hongo, Bunkyo-ku, Tokyo, 113-8421, Japan, and the Department of Entomology & Nematology and Comprehensive Cancer Research Center[3], University of California, Davis, CA 95616

[1]To whom correspondence should be address: Alan R. Brash, Ph.D., Department of Pharmacology, Vanderbilt University School of Medicine, 23rd Ave at Pierce, Nashville, TN 37232-6602. Tel: 615-343-4495, Email: alan.brash@vanderbilt.edu

Running title: Epoxide hydrolases and epidermal linoleate metabolism

Abstract

Lipoxygenase-catalyzed oxidation of the essential fatty acid linoleate represents a vital step in construction of the mammalian epidermal permeability barrier. Analysis of epidermal lipids indicates the linoleate is converted to a trihydroxy derivative by hydrolysis of an epoxy-hydroxy precursor. We evaluated different epoxide hydrolase (EH) enzymes in the hydrolysis of skin-relevant fatty acid epoxides and compared the products to those of acid-catalyzed hydrolysis. In the absence of enzyme, exposure to pH 5 or pH 6 at 37 °C for 30 min hydrolyzed fatty acid allylic epoxyalcohols to four trihydroxy products. By contrast, human soluble epoxide hydrolase (EPHX2) and human or murine epoxide hydrolase-3 (EPHX3) hydrolyzed *cis* or *trans* allylic epoxides to single diastereomers, identical to the major isomers detected in epidermis. Microsomal epoxide hydrolase (EPHX1) was inactive with these substrates. At low substrate concentrations (<10 μM), EPHX2 hydrolyzed 14,15-epoxyeicosatrienoic acid (14,15-EET) at twice the rate of the epidermal epoxyalcohol 9*R*,10*R*-*trans*-epoxy-11*E*-13*R*-hydroxy-octadecenoic acid, whereas human or murine EPHX3 hydrolyzed the allylic epoxyalcohol at 31-fold and 39-fold higher rate, respectively. These data implicate the activities of EPHX2 and EPHX3 in production of the linoleate triols detected as end products of the 12R-lipoxygenase pathway in the epidermis and implicate their functioning in formation of the mammalian water permeability barrier.

Keywords: Linoleic acid, lipoxygenase, epoxide hydrolase, fatty acid epoxide, trihydroxy-linoleate, 14,15-EET, epidermis, ichthyosis

Abbreviations

APCI-LC-MS, atmospheric pressure chemical ionization liquid chromatography mass spectrometry; Cer-EOS esterified omega-hydroxyacyl-sphingosine; Cer-OS, omega-hydroxyacyl-sphingosine; DCM, dichloromethane; DMP, dimethoxypropane or dimethoxypropyl; EET, epoxyeicosatrienoic acid; EH, epoxide hydrolase; EH3, epoxide hydrolase-3 (EPHX3); eLOX3, epidermal lipoxygenase-3; HPODE, hydroperoxy-octadecadienoic acid; LC-MS, liquid chromatography-mass spectrometry; LOX, lipoxygenase; mCPBA, m-chloroperoxybenzoic acid; mEH, microsomal epoxide hydrolase (EPHX1); PFB, pentafluorobenzyl; RP-HPLC, reversed-phase high pressure liquid chromatography; sEH, soluble epoxide hydrolase (EPHX2); SP-HPLC, straight-phase high pressure liquid chromatography.

Introduction

Among the gene products required for formation of the mammalian epidermal water barrier are the two lipoxygenase enzymes, 12*R*-lipoxygenase (12*R*-LOX) and epidermal lipoxygenase-3 (eLOX3) (1, 2). Inactivating mutations in either enzyme leads to trans-epidermal water loss and the fish skin symptoms of congenital ichthyosis in afflicted families (3) and to neonatal lethality in mice (2). The 12R-LOX/eLOX3 substrate in the epidermis is the essential fatty acid linoleate, which is esterified to the omega-hydroxyl of the very long chain fatty acid component of the unique epidermal acylceramides (Cer-EOS) (4, 5). Products of the actions of 12R-LOX and eLOX3 are detectable in the outer epidermis as epoxy-hydroxy (epoxyalcohol) derivatives of the ceramide-linoleate ester (6). Oxidation of the linoleate moiety is proposed to facilitate hydrolysis of the ester bond, freeing the omega hydroxyl of the ceramide for coupling to cross-linked proteins, a vital step in sealing the water barrier (6).

Recent evidence suggests that this oxidative pathway in the outer epidermis is extended by transformation of the epoxyalcohol formed by the action of 12R-LOX and eLOX3 to a trihydroxy derivative (7), Fig. 1A. For illustrative purposes, (the relevance of which will be evident later with presentation of Results), the pattern of linoleate triols previously reported to be esterified in Cer-EOS of pig and human epidermis is shown in Fig. 1B (7). It is a central tenet of the hypothesis governing the involvement of the LOX pathway in epidermal barrier construction that oxidation of the linoleate ester has a disruptive effect on the lipid environment and that this facilitates esterase-catalyzed removal of the (oxidized) linoleate (6). Thus, implicating the linoleate triol in the pathway supports and extends the hypothesis because the triols have the high polarity needed for disruption of the lipid environment, facilitating cleavage of the oxidized Cer-EOS for covalent coupling of the free Cer-OS to protein. The relative polarities of linoleate, its 9-hydroperoxide, the epoxyalcohol, and a linoleate triol are shown on Fig. 1A as the trend towards a reduced logP partition coefficient, with formation of the triol making a major impact.

The above considerations bring in the potential involvement of one or more epoxide hydrolases in producing the distinctive patterns of linoleate triols previously observed in pig and human epidermis and illustrated in Fig. 1B (7). The two well studied enzymes in mammalian biology are microsomal epoxide hydrolase (mEH, EPHX1), and soluble epoxide hydrolase (sEH, EPHX2) (8), and in this paper we evaluate both for their ability to hydrolyze the relevant fatty acid epoxides. The EH gene family also includes EH3, EH4, and peg1/MEST (9). Peg1/MEST (paternally expressed gene 1/mesoderm specific transcript) is an unlikely candidate; it is an imprinted gene with roles in development (10) and not so far shown to have epoxide hydrolase activity. EH4 is similarly unstudied as an epoxide hydrolase; the main site of its gene expression is the CNS (11), and more recently it is attributed a role in sebocyte lipid droplet biogenesis (12). The third additional candidate is EH3, which is known to hydrolyze fatty acid *cis*-epoxyeicosatrienoic acids (EETs, which have proposed roles in epidermal differentiation (13)), and EH3 is highly expressed in the skin (14); moreover, the highest expression of EH3 mRNA is in the outer epidermis where the water permeability barrier is formed (15). From comparison of expression patterns of candidate genes with disease-related gene clusters EPHX3 is also recognized as a potential ichthyosis gene (16). For all these reasons EH3 was selected along with mEH and sEH for evaluation of their catalytic activity with epidermis-related fatty acid epoxides.

Experimental Procedures

Materials - Linoleic acid, methyl linoleate and linoelaidic acid were purchased from Nu-Chek Prep Inc (Elysian, MN). 9*R*-HPODE was prepared using *Anabaena* 9*R*-LOX (6). Epoxyalcohol and triol derivatives of 9-hydroperoxy-linoleic acid were prepared as previously described (17). Pentafluorobenzyl bromide (PFBBr), *p*-toluene sulfonic acid, pyridinium *p*-toluenesulfonate, diisopropylethylamine (DIPE), 2,2-dimethoxypropane (DMP) and trimethylamine were obtained from (Sigma-Aldrich, St. Louis, MO).

p-Toluenesulfinic acid was obtained by acidification of aqueous solutions of the commercially available sodium salt with HCl (18). The mixture of eight deuterated linoleate triols was prepared by autoxidation of [$^2H_4$]linoleic acid as previously described (7). [$^2H_8$]14,15-dihydroxy-eicosatrienoic acid was prepared by mCPBA treatment of d8-arachidonic acid, isolation of the 14,15-EET, and acid hydrolysis to the d8-14,15-diol. Two synthetic trihydroxy derivatives of linoleic acid, 9*R*,10*R*,13*R*-trihydroxy-11*E*-octadecenoic acid (triol-1) and the 9*R*,10*S*,13*R* isomer (triol-3), were prepared by total synthesis using methodology to be described elsewhere.

Derivatization procedures - PFB esters were prepared by dissolving the d4 standards or triol analyte in 20 µl acetonitrile, 20 µl PFBBr in acetonitrile (1:19, v/v) and 20 µl of DIPE in acetonitrile (1:9, v/v). The solution is incubated at R.T. under argon for 30 min then evaporated to dryness under nitrogen. Acetonide (dimethoxypropyl, DMP) derivatives of the triols were prepared by treatment of the fatty acid PFB ester with 20 µl of 1 mM pyridinium p-toluenesulfonate in acetone/DMP (1:1 by volume) for 30 min at RT. Samples were then taken to dryness under a stream of nitrogen and redissolved in SP-HPLC solvent (hexane/IPA, 100:1 v/v) for subsequent HPLC-UV or LC-MS analysis.

*Preparation of 9R,10R-trans-epoxy-13R-hydroxy-octadeca-11E-enoic acid (**1**), and 9R,10S-cis-epoxy-13R-hydroxy-octadeca-11E-enoic acid (**2**) (Fig. 2A)* – These allylic epoxides were isolated following hematin treatment of 9*R*-HPODE as described (17). Briefly, 9R-HPODE was prepared in 5 – 10 mg quantities using recombinant *Anabaena* 9R-LOX (19) and converted by hematin treatment to a mixture of products that were separated by SP-HPLC. *trans*-epoxyalcohol **1** is recovered in about 10% yield and the more minor *cis*-epoxyalcohol **2** in ~3% yield. The products were quantified by conversion of an aliquot of approximately 50 µg to the PFB ester and, after SP-HPLC purification, quantified using the UV chromophore at 263 nm in EtOH (ε = 570 M^{-1} cm^{-1}, unpublished data); although this could lead to a slight

underestimate of the free acid concentration due to incomplete recovery, the method was considered accurate to within 10%.

*Preparation of 12,13-trans-epoxy-octadeca-9E-enoic acid ("trans-epoxide **3**") (Fig. 2B)* – 20 mg of linoelaidic acid, the 9*E*,12*E* geometric isomer of linoleic acid, was epoxidized using equimolar mCPBA in dichloromethane for 30 min at room temperature. The two major products, the 12,13- and 9,10-*trans*-epoxides were separated on SP-HPLC using a semi-preparative Beckman 5 μm Ultrasphere silica column (250×10 mm) with a solvent of hexane/IPA/glacial acetic acid (100/0.4/0.02), a flow rate of 5.0 ml/min; the peaks were detected by UV monitoring at 205 nm and eluted at 25.8 min (12,13-*trans*-epoxy-) and 31.8 min (9,10-*trans*-epoxides). The products were quantified by weighing.

*Preparation of 12,13-cis-epoxy-octadeca-9E-enoic acid ("cis-epoxide **4**") (Fig. 2B)* – This epoxide was prepared by initial isomerization of methyl linoleate (20 mg) to a mixture of the non-conjugated 9E,12Z and 9Z,12E isomers (18) which were isolated by silver ion chromatography. Following epoxidation of the 9E,12Z and 9Z,12E isomers with mCPBA, the products were separated by SP-HPLC using a Thomson silica column, 5 μm 4.6 × 250mm, a solvent of hexane /IPA (100:0.2), and a flow rate of 0.5ml/min. The mixture chromatographed as three peaks in 1:3:2 ratio in order of elution. From preliminary studies using a model compound, 6E,9Z-pentadecadiene (20), we found that mCPBA favored epoxidation of the *cis* double bond by 2:1 over *trans*. From this, and knowing that on SP-HPLC 12,13-epoxy-linoleates elute before the 9,10-epoxides (21), we could interpret the 1:3:2 ratio as an early-eluting 12,13-*trans*-epoxide (area of 1), a mixture of 12,13-*cis*-epoxide (area of 2) and 9,10-*trans*-epoxide (area of 1), and lastly a peak of the 9,10-*cis*-epoxide (area of 2). This was later confirmed by NMR. The mixture of 12,13-*cis*-epoxy-9*E* and 9,10-*trans*-epoxy-12*Z* eluted at 13.1 min and was resolved by silver ion chromatography using a Waters 5μm 4.6 × 250 mm column in the Ag^+ form with a solvent of hexane /IPA (100:1), and a flow rate of 0.5ml/min. The first eluting peak, 12,13-*cis*-epoxy-octadeca-9*E*-enoate, at ~9 min retention

time was collected and alkali-hydrolyzed to the free acid. It was quantified by HPLC peak area (205 nm) in comparison to *trans*-epoxide 3, yield 175 µg. NMR in C_6D_6 showed, δ ppm: 5.52, 1H, ddd, $J_{9,10}$ = 15.4 Hz, H9; 5.46, 1H, ddd, $J_{9,10}$ = 15.4 Hz, H10; 2.87, 1H, dt, $J_{12,13}$ = 4.1 Hz, H12; 2.75, 1H, dt, $J_{12,13}$ = 4.2 Hz, H13; 2.27, 1H, dd, H11a; 2.11, 1H, ddd, H11b; 2.04, 1H, t, H2; 1.55 – 1.05, 18H, m, H3, 4, 5, 6, 7, 14, 15, 16, 17; 0.85, 3H, t, H18.

Analysis of the pH sensitivity of allylic epoxides - 9*R*,10*R*-*trans*-epoxy-13*R*-hydroxy-octadeca-11*E*-enoic acid ("*trans*-epoxyalcohol **1**") and 9*R*,10*S*-*cis*-epoxy-13R-hydroxy-octadeca-11E-enoic acid ("*cis*-epoxyalcohol **2**") (2 µl in EtOH, ~1 µg) were incubated in 48 µl of pH 5, pH 6, pH 7 and pH 8 0.1 M phosphate buffers for times up to 1 h at 37 °C. After incubation at 37 °C, 50 µl of cold acetonitrile was added and the samples were placed on ice and analyzed in turn (10% aliquots, lowest pH first) by RP-HPLC-UV using a Kinetex 2.6-µm C18 column (100 × 3 mm) with a 0.5 µm PEEK precolumn microfilter, a solvent of CH_3CN/H_2O/HAc (45/55/0.01) and flow rate of 0.4 ml/min with UV monitoring at 205 nm. To suppress ionization and achieve consistent retention times of the pH 7 and pH 8 samples, 2 µl of 10-fold diluted glacial acetic acid was added immediately prior to injection.

The non-enzymatic hydrolysis products from the pH 5 and pH 6 conditions were collected using a Waters Symmetry C18 column, 4.6 × 250 mm, a solvent of CH_3CN/H_2O/HAc (50/50/0.01), and a flow rate of 1 ml/min, giving a retention time of 4.5~4.8 min and 4.2~4.4 min for the triol products from *trans*-epoxyalcohol **1** and *cis*-epoxyalcohol **2**, respectively (detected at 205 nm). The products were converted to the PFB ester DMP derivative and analyzed by APCI-LC-MS using a TSQ Vantage instrument (Thermo Scientific) with a Waters Alliance 2690 HPLC system, and a Kinetex 100A 2.6 µm Hilic column (100×2.1 mm) with a solvent of hexane/IPA (100:1, v/v), and a flow rate of 0.4 ml/min. The APCI vaporizer temperature was set to 300 °C, and the electrospray ionization probe temperature was set to

150 °C with selected ion monitoring of negative ions at m/z 369 for the unlabeled triol derivatives and m/z 373 for a mixture of eight d4-triol standards prepared as described (7).

Preparation of the human EH3, sEH and mEH - A full-length sequence of human EH3 (GenBank Accession BC132960) was PCR-amplified from a template plasmid obtained from the Integrated Molecular Analysis of Genomes and their Expression (I.M.A.G.E.) Consortium (Clone ID 40146982) through Open Biosystems. The PCR reactions were performed using KOD Hot Start polymerase (EMD Millipore) with primers EH3BglATG (5'- GAAGATCTATGCCGGAGCTGGTGGTGACCG-3') and EH3stopEco (5'-CGGAATTCCTAGTCCAGCAGGTCTTGCAAGAAGGC-3') following the manufacturer's recommended procedures. The use of primers EH3BglATG and EH3stopEco placed BglII and EcoRI sites at the 5'- and 3'-ends of the coding sequence, respectively. The amplicon (1.1 kbp) was inserted into the cloning vector pCR-Blunt II-TOPO (Invitrogen) and sequenced in both directions in order to confirm the authenticity of the sequence. Subsequently, the 1.1 kbp-long insert was excised by digestion with BglII and EcoRI, and then ligated using T4 DNA ligase (New England BioLabs) into the BglII and EcoRI sites of the baculovirus transfer vector pAcUW21 in order to generate the recombinant baculovirus Ac-hEH3 that expresses the human EH3 following published procedures pAcUW21-hEH3 (22). The human sEH and mEH were cloned in similar baculoviruses previously (23, 24). Human sEH, mEH and EH3 were produced in a baculovirus expression system as previously described (23). Human sEH was purified by affinity chromatography (25), mEH was partially purified by chromatography (26), and a microsomal cell extract was used as a source of human EH3. The human sEH, mEH, and EH3 preparations were 97%, 80% and 4% pure, respectively, as judged by sodium dodecyl sulfate-polyacrylamide gel electrophoresis and scanning densitometry. The activity of the purified enzymes were tested using radioactive surrogate substrates (27). The human sEH and human EH3 activities were tested using [^{3}H]-*trans*-diphenyl-propene oxide as substrate, and found to be 7,100 and 48 nmol.min^{-1}.mg^{-1},

respectively. The human mEH activity was measured with [^{3}H]-*cis*-stilbene oxide, and found to be 490 nmol.min^{-1}.mg^{-1}.

Mouse EH3 protein expression - Three different constructs of murine EH3 sequence (see Results) we refer to as full-length, N-truncated and N-truncated＋7aa-insert, were ordered with an additional N-terminal $(His)_6$ tag from Genewiz (South Plainfield, NJ); the full-length sequence was codon-optimized for expression in Sf9 cells, whereas the truncated constructs were ordered with the natural sequences. The three constructs were first tested in *E. coli* in a pET plasmid only to see no enzyme activity, so expression was tested in Sf9 cells in the pVL1393 vector (PharMingen, San Diego, CA). Expression was carried out using the AB Vector Proeasy^{TM} baculovirus expression system. Cell lysates were tested for epoxide hydrolase activity and paradoxically, the codon-optimized full-length cDNA failed to express with enzyme activity, and therefore further experiments were carried out with the N-truncated proteins. Although lysates of the N-truncated constructs had activity, no band was evident on SDS-PAGE and the activity failed to solubilize using a number of detergents, so cell lysates were used in our experiments.

Enzymatic activity and pH activity profile with model cis and trans epoxy standards – Enzymatic hydrolysis of 12,13-*trans*-epoxy-octadeca-9*E*-enoic acid ("*trans*-epoxide **3**") and 12,13-*cis*-epoxy-octadeca-9*E*-enoic acid ("*cis*-epoxide **4**") (~ 0.75 μg) were compared with two different epoxide hydrolases, human sEH (purified protein:100 ng), and human EH3 used as cell lysates containing 54 μg, of protein, respectively. Incubations were conducted for 60 min at 37 °C in a 0.5 ml Eppendorf tube containing 12μl of enzyme lysate, 1 μl of epoxyalcohol substrate in EtOH (0.75 μg) made up to a total volume of 50 μl with phosphate buffer (0.1 mM, pH 8.0). The pH activity profiles using the model *trans*-epoxide **3** (50 μM) were conducted in 50 μl aliquots of 0.1 M phosphate buffers at pH, 5, 6, 7, or 8 for 30 min at 37°C with human sEH and human EH3. Reactions were terminated after 60 min by addition of an equal volume of acetonitrile. Then the samples were centrifuged for 10 min at 14,000 rpm, the

supernatant was injected into RP-HPLC used a Kinetex 2.6-μm C18 column (100 × 3 mm) with a 0.5 μm PEEK precolumn microfilter, a solvent of CH_3CN/H_2O/HAc (45/55/0.01) and flow rate of 0.4ml/min, giving a retention time of 2.2 and 2.3 min for diol products from *trans*-epoxide **3** and *cis*-epoxide **4** (detected at 205 nm). Immediately prior to HPLC of the samples approximately 2 μl of 10-fold dilute glacial acetic acid was added to suppress ionization and achieve consistent retention times, mixed, and the aliquot injected immediately.

Incubations of allylic epoxyalcohols with epoxide hydrolases - Enzymatic hydrolysis of *trans*-epoxyalcohol **1** and *cis*-epoxyalcohol **2** (~1 μg) was examined with five different epoxide hydrolases, human sEH (purified protein:100 ng), human EH3, N-truncated murine EH3, and N-truncated＋7aa-insert murine EH3 used as cell lysates containing 54 μg, 74 μg, and 68 μg of protein, respectively), and human (purified protein:100 ng). Incubations were conducted for 60 min at 37 °C in a 0.5 ml Eppendorf tube containing 12 μl of enzyme lysate, 1 μg of epoxyalcohol substrate in EtOH (1 μl) made up to a total volume of 50 μl with Tris buffer (10 mM, pH 8.0) containing NaCl (100 mM), EDTA (1 mM) and gelatin (0.1% w/v). Reaction was terminated after 60 min by addition of an equal volume of acetonitrile. Then the samples were taken to dryness under a stream of nitrogen and redissolved with 100 μl CH_3CN/H_2O/HAc (60/40/0.01). After centrifugation for 10 min at 14,000 rpm, the supernatant was injected into RP-HPLC with a Waters Symmetry C18 column, 4.6 × 250 mm, a solvent of CH_3CN/H_2O/HAc (60/40/0.01), and flow rate of 0.75ml/min, giving a retention time of 4.0 and 3.7 min for triol products from RRR *trans*- and RSR *cis*-epoxyalcohol: the peaks (205 nm) were collected manually and subsequently derivatized for LC-MS analysis as described above.

RESULTS

Acid-catalyzed hydrolysis of linoleate allylic epoxyalcohols – Prior to assessing the characteristics of enzymatic hydrolysis of skin-related linoleate epoxyalcohols it is important to describe their sensitivity to non-enzymatic hydrolysis. The pH of the mammalian outer epidermis is slightly acidic (the pH for human skin lies in the broad range 4.0-7.0, (28, 29)) and the epoxyalcohols derived via 12R-LOX and eLOX3 catalysis include an allylic epoxide structure that should be acid sensitive. Therefore, we carefully assessed the effects of a mildly acidic environment on the hydrolytic degradation of epidermal epoxyalcohols. Incubated in pH 8 or pH 7 buffer, the skin-related *trans*-epoxyalcohol **1** was not hydrolyzed over the course of 30 min at 37 °C (Fig. 3, A and B), whereas non-enzymatic hydrolysis was about 70% complete at pH 6 (Fig. 3C) and full hydrolysis occurred after 30 min in pH 5 buffer (Fig. 3D). The *cis*-epoxyalcohol **2** showed essentially the same pH sensitivity, being fully hydrolyzed after 30 min at 37 °C in pH 5 buffer (Fig. 3, E-H).

The individual triol products of these non-enzymatic hydrolyses were identified by LC-MS of the PFB ester DMP derivative, a method that allows assignment of eight separate triol isomers, illustrated in Fig. 4A(7) (and the same HPLC method illustrated in Fig. 1B of the Introduction). Non-enzymatic hydrolysis of the *trans*-epoxyalcohol **1** at pH 6 or pH 5 gave four triol products (designated here as triols 1 – 4) as expected from bidirectional attack of water at both C-10 and C-12 (Fig. 4, B and C, and Fig. 5A); in three separate experiments the relative proportions of triols 1 – 4 averaged 25:14:30:31, respectively (Fig. 5A), similar to the result using 0.1% aqueous glacial acetic acid which averaged 28:18:26:28. In contrast to the four prominent triols formed from the *trans* epoxide, the corresponding *cis* epoxyalcohol **2** gave one prominent hydrolysis product in 65% relative abundance along with three minor triols (proportions 65:9:14:12, respectively, Fig. 4D, 4E, and Fig. 5B), similar to the proportions using 0.1% aqueous glacial acetic acid (63:9:14:14).

Preparation of mouse EH3 epoxide hydrolase – Analysis of the EPHX3 sequences in GenBank shows that rodent EH3 is expressed with an additional 57 amino acids on the N-terminus and that mouse EH3 is found in a second isoform that contains a 7 amino acid insert after position 138 (Fig. 6). We elected to express one construct containing the full-length sequence including the 7 aa insert, and two variants (+/- the 7 aa insert) with the rodent-specific 57 aa N-terminal sequence removed (Fig. 6). Heterologous expression of these constructs in several strains of *E. coli* gave a strong band at the expected molecular mobility on SDS-PAGE but the proteins were insoluble and completely lacking in catalytic activity. Expression of active enzyme in Sf9 insect cells was successful with both of the truncated forms of the enzyme, whereas the full length construct exhibited no activity. Although activity was readily measurable for the N-terminally shortened constructs the expression level was insufficient to visualize the EH3 protein on SDS-PAGE. Lysates of EH3-expressing Sf9 cells were used for all experiments. Similar findings to the above were reported for human EH3 expression in *E. coli* and Sf9 cells (14), and similarly we used Sf9 cell lysates for assessment of human EH3 activity.

Enzymatic hydrolysis of model linoleate epoxides- Both sEH and EH3 are known to efficiently hydrolyze the arachidonate-derived *cis*-epoxyeicosatrienoic acids and sEH is known also to metabolize *trans*-EETs (EETs) (30). We were interested in comparing the hydrolase activity with *cis* and *trans* epoxides of otherwise identical structure, and as we did not have the *trans*-EET analogues available, we prepared model linoleate epoxides **3** and **4** for these experiments. These non-allylic epoxides are chemically stable at pH 5 or 6, which would prove useful for comparing the hydrolase activities of sEH and EH3 at the slightly acidic pH values typical of human epidermis.

As an initial screen for epoxide hydrolase activity comparing *trans*-epoxide **3** with *cis*-epoxide **4** the substrates were incubated for 1 h at 37 °C with human sEH, human EH3 and one of the mouse EH3 constructs. The concentrations of enzymes used were those known to metabolize EETs. Under these

conditions, recombinant sEH (100 ng/ml) partially hydrolyzed both the *trans* and *cis* epoxide, showing a preference for the *trans* epoxide **3** (Fig. 7B), similar to reported properties with *trans* and *cis* EETs (30). Human EH3 and mouse EH3 showed similar activities, hydrolyzing both epoxides **3** and **4**, with a preference for *trans* **3** (Fig. 7C and D). Using *trans*-epoxide 4 as substrate, the pH profiles of activity of sEH and EH3 were compared at pH 5 – pH 8 (Fig. 8).

Enzymatic hydrolysis of allylic linoleate epoxides- *trans*-Epoxyalcohol **1** and *cis*-epoxyalcohol **2** were tested with human sEH, human EH3, murine EH3 (both the N-truncated form and the N-truncated＋7aa-insert). Hydrolysis products of the epoxyalcohol, triol, was collected and derivatized to PFB ester, then to DMP for further analysis. Fig. 9 compares the RP-HPLC profiles of linoleate allylic epoxyalcohol substrate and the more polar hydrolysis products. Under the conditions used, *trans*-epoxyalcohol **1** was completely hydrolyzed using human sEH, human EH3, and N-truncated murine EH3 and mostly hydrolyzed using N-truncated＋7aa-insert murine EH3. *cis*-epoxyalcohol **2** was hardly hydrolyzed using human EH3, N-truncated murine EH3 N-truncated＋7aa-insert murine EH3 and ~30% hydrolysis was observed using human sEH. Human mEH did not hydrolyze *trans*-epoxyalcohol **1** or *cis*-epoxyalcohol **2** (Fig. 9).

Identification of the enzymatic hydrolysis products of linoleate allylic epoxyalcohols – Applying the same LC-MS assay used to characterize the mixtures of triols formed non-enzymatically, human sEH, human EH3, murine EH3 (both the N-truncated form and the N-truncated＋7aa-insert) are shown to convert *trans*-epoxyalcohol **1** exclusively to triol-3 (Fig. 10, A - E). Likewise, the hydrolysis of *cis*-epoxyalcohol 2 by human sEH and human EH3 exclusively gave triol-1 (Fig. 10, F and G).

Comparison of the rates of EET and linoleate allylic epoxide hydrolysis by sEH and EH3 - Both sEH and EH3 are known to metabolize EET-type epoxides (14). In the case of the well-studied sEH, the reports

include the metabolism of both *cis*- and *trans*-EETs (30) and the hydrolysis of the linoleate 9,10- and 12,13-*cis*-epoxides (31). Here we compared the rates of hydrolysis of 14,15-EET and *trans*-epoxyalcohol-**1** under identical incubation conditions with sEH and EH3. The hydrolysis products were quantified by LC-MS using deuterated internal standards prepared for the study and the results are illustrated in Fig. 11. Using the rate versus substrate concentration data (Fig. 11), the turnover rates were calculated at low substrate concentration (1 μM) to observe first-order behavior. Human sEH showed 2.1-fold higher activity in the hydrolysis of *cis*-14,15-EET over epoxyalcohol **1** (Fig. 11A). By contrast, human and murine EH3 showed 31-fold and 39-fold differences, respectively, with the preference reversed in favor of epoxyalcohol **1** hydrolysis over *cis*-14,15-EET (Fig. 11B and C).

DISCUSSION

Epoxide hydrolases implicated in epidermal water barrier formation- The aim of this study was to investigate the catalytic activities of epoxide hydrolase enzymes potentially involved in formation of the epidermal permeability barrier. So far, no epoxide hydrolase has been tested with substrates directly relevant to the LOX epidermal permeability pathway. Herein we demonstrate that the epoxide hydrolases sEH and EH3 enzymatically hydrolyze *trans*-epoxyalcohol **1** (skin-related allylic epoxide) to RSR triol-3, the most abundant triol isomer in human and porcine epidermis (7) (cf. Fig. 1B), and the *cis*-epoxyalcohol **2** is hydrolyzed to triol-1. This is consistent with the mechanism whereby epoxide hydrolase inserts oxygen from water (via the active site aspartate) with reversal of configuration (Fig. 10). Our results are compatible with a significant role of the epoxide hydrolases, EH3 and sEH, in epidermal LOX pathway. There is compelling experimental and analytical support for a role of an epoxide hydrolase in skin barrier formation, although on the basis of the lack of a skin phenotype in the single knockouts of sEH and EH3 already reported (32, 33) there is functional redundancy of epoxide hydrolases in the epidermis. Soluble EH is well expressed in skin (34), and transcriptome analysis of human granular keratinocytes identified

EH3 as highly expressed in the outermost cells of human epidermis (20-fold over basal cells) (15). Also, co-expression analysis of mouse and human disease-related gene clusters identified EH3 as a predicted ichthyosis gene (p value 10^{-14}) (16). In fact, on the basis of the tissue expression of mouse EH3, highest in skin, Decker et al concluded that "Based on [expression], it is tempting to speculate on a potential role of EH3 in barrier formation" (14).

Analysis of the relative rates of hydrolysis of 14,15-EET and epoxyalcohol **1** at very low substrate concentrations (the initial slopes of the rate *versus* substrate concentration lines reflecting the ratio of kcat/KM) showed that sEH hydrolyzes each substrate within the same order of magnitude (2-fold more efficiently in favor of 14,15-EET). By contrast, both human and mouse EH3 greatly favor the *trans* epoxyalcohol **1**, by factors of 31- and 39-fold respectively. Also, Figure 9 shows that EH3 has a great preference for the *trans*-allylic epoxyalcohol **1** over the *cis* analog **2**, further supporting its potential relevance to the hydrolase activity in the 12R-LOX/eLOX3 pathway.

Reported non-enzymatic hydrolysis of other fatty acid epoxides – Although to the best of our knowledge the acid instability of the arachidonic acid-derived EETs or the equivalent linoleate analogues has not been studied in detail, one of the chemical procedures for their hydrolysis to diols involves treatment with 70% perchloric acid (35), i.e. the epoxides are moderately stable and strongly acidic conditions or exceptionally long incubation times are required for their complete hydrolysis. An exception is 5,6-EET, in which the free ionized carboxyl at C-1 facilities hydrolysis and 5,6-EET is chemically unstable at pH 8.0 and 25 ℃; 5,6-EET was hydrolyzed to a diol within 1.5 h and complete hydrolysis was observed within 7.5 h (36). At the extreme end of the spectrum of instability of fatty acid epoxides are leukotriene A_4, with its epoxide moiety allylic to a conjugated triene and with an estimated half-life of 3.6 seconds at pH 7.4 and 25 °C (37); and the fatty acid allene oxides, with a double bond impinging directly on the epoxide, have a reported half-life of 30 - 40 seconds at pH 7.4 and 0 °C (38, 39).

Among the fatty acid epoxyalcohols (including the hepoxilins (40)) it is recognized that the hepoxilin B analogues with the alcohol group between the epoxide and a double bond are stable for short periods at pH 3(41), whereas the hepoxilin A-type, which are analogues of the epoxyalcohols **1** and **2** studied here, can survive only briefly at pH 3 (1). Herein we refine this understanding by showing the hydrolysis of **1** and **2** at pH 5 (complete within 30 min at 37°C) and pH 6, which gives about 50% hydrolysis under the same conditions. Most significantly, the pattern of non-enzymatic hydrolysis products of the epoxyalcohol of the LOX pathway in the epidermis (epoxyalcohol **1**) gives four triols in 14%, 25%, 30% and 30% relative abundance (Fig. 4 and Fig. 5). By contrast, the actions of sEH and EH3 give a single main triol, the same one that is prominent in pig and human epidermis (cf. Fig. 1). This evidence greatly strengthens the argument that epoxide hydrolase(s) participate in the production of the linoleate triols detected in the mammalian epidermis. Some doubt remains on the enzymatic or non-enzymatic origin of triol-1 in the epidermis. Under very mild acidic conditions (pH 5, pH 6) the *cis*-epoxyalcohol 2 is hydrolyzed non-enzymatically predominantly to triol-1 (and exclusively to triol-1 by the action of EH enzymes), leaving open the basis of its synthesis in the skin.

Concluding remarks - The current studies along with earlier findings are consistent with a role for epoxide hydrolase in the 12R-LOX/eLOX pathway in the epidermis. The next steps needed to test the postulated involvement in the formation of esterified linoleate triols and in epidermal barrier function under in vivo conditions will include the comparison of single or multiple EPHX knockout mice. This will define the functioning of specific epoxide hydrolases in the production of esterified linoleate triols, their significance to the epidermal permeability barrier, and contribute to development of an integrated model of epidermal barrier formation. Notably, loss of the covalently bound ceramides as occurs with 12R-LOX deficiency is similarly a feature of the gene inactivation of eLOX3 (42), P450 CYP4F22 (that omega-hydroxylates Cer to give Cer-OS) (43), PNPLA1 (that couples linoleate to Cer-OS) (44, 45), and CGI-58 (ABHD5, that facilitates the formation of CER-EOS) (46). Taken together, the importance of this

work is for the basic understanding of a vital process for mammalian survival ("that permits terrestrial life" (47)), and for understanding the disease-related pathology and symptomology associated not only with the relatively rare cases of ARCI (48) but also symptomatic of such common skin conditions as atopic dermatitis, a huge clinical issue (49, 50).

ACKNOWLEDGEMENTS

Research reported in this publication was supported by the National Institute of Arthritis and Musculoskeletal and Skin Diseases of the National Institutes of Health under Award Number AR-51968 (to ARB), and by NIH grant GM-115722 (to GAS), and NIEHS grant R01-ES002710 and Superfund Research Program P42 ES04699 (to BDH). The content is solely the responsibility of the authors and does not necessarily represent the official views of the National Institutes of Health.

REFERENCES

1. Muñoz-Garcia, A., C. P. Thomas, D. S. Keeney, Y. Zheng, and A. R. Brash. 2014. The importance of the lipoxygenase-hepoxilin pathway in the mammalian epidermal barrier. *Biochim. Biophys. Acta* **1841**: 401-408.

2. Krieg, P., and G. Furstenberger. 2014. The role of lipoxygenases in epidermis. *Biochim. Biophys. Acta* **1841**: 390-400.

3. Elias, P. M., M. L. Williams, W. M. Holleran, Y. J. Jiang, and M. Schmuth. 2008. Pathogenesis of permeability barrier abnormalities in the ichthyoses: inherited disorders of lipid metabolism. *J. Lipid Res.* **49**: 697-714.

4. Wertz, P. W., and D. T. Downing. 1983. Acylglucosylceramides of pig epidermis: structure determination. *J. Lipid Res.* **24**: 753-758.

5. Bowser, P. A., D. H. Nugteren, R. J. White, U. M. Houtsmuller, and C. Prottey. 1985. Identification, isolation and characterization of epidermal lipids containing linoleic acid. *Biochim. Biophys. Acta* **834**: 419-428.

6. Zheng, Y., H. Yin, W. E. Boeglin, P. M. Elias, D. Crumrine, D. R. Beier, and A. R. Brash. 2011. Lipoxygenases mediate the effect of essential fatty acid in skin barrier formation: a proposed role in releasing omega-hydroxyceramide for construction of the corneocyte lipid envelope. *J. Biol. Chem.* **286**: 24046-24056.

7. Chiba, T., C. P. Thomas, M. W. Calcutt, W. E. Boeglin, V. B. O'Donnell, and A. R. Brash. 2016. The Precise Structures and Stereochemistry of Trihydroxy-linoleates Esterified in Human and Porcine Epidermis and Their Significance in Skin Barrier Function: IMPLICATION OF AN EPOXIDE HYDROLASE IN THE TRANSFORMATIONS OF LINOLEATE. *J. Biol. Chem.* **291**: 14540-14554.

8. DuTeaux, S. B., J. W. Newman, C. Morisseau, E. A. Fairbairn, K. Jelks, B. D. Hammock, and M. G. Miller. 2004. Epoxide hydrolases in the rat epididymis: possible roles in xenobiotic and endogenous fatty acid metabolism. *Toxicol. Sci.* **78**: 187-195.

9. Decker, M., M. Arand, and A. Cronin. 2009. Mammalian epoxide hydrolases in xenobiotic metabolism and signalling. *Arch. Toxicol.* **83**: 297-318.

10. Lefebvre, L., S. Viville, S. C. Barton, F. Ishino, E. B. Keverne, and M. A. Surani. 1998. Abnormal maternal behaviour and growth retardation associated with loss of the imprinted gene Mest. *Nat. Genet.* **20**: 163-169.

11. Lord, C. C., G. Thomas, and J. M. Brown. 2013. Mammalian alpha beta hydrolase domain (ABHD) proteins: Lipid metabolizing enzymes at the interface of cell signaling and energy metabolism. *Biochim. Biophys. Acta* **1831**: 792-802.

12. Dahlhoff, M., T. Frohlich, G. J. Arnold, U. Muller, H. Leonhardt, C. C. Zouboulis, and M. R. Schneider. 2015. Characterization of the sebocyte lipid droplet proteome reveals novel potential regulators of sebaceous lipogenesis. *Exp. Cell Res.* **332**: 146-155.

13. Ladd, P. A., L. Du, J. H. Capdevila, R. Mernaugh, and D. S. Keeney. 2003. Epoxyeicosatrienoic acids activate transglutaminases in situ and induce cornification of epidermal keratinocytes. *J. Biol. Chem.* **278**: 35184-35192.

14. Decker, M., M. Adamska, A. Cronin, F. Di Giallonardo, J. Burgener, A. Marowsky, J. R. Falck, C. Morisseau, B. D. Hammock, A. Gruzdev, D. C. Zeldin, and M. Arand. 2012. EH3 (ABHD9): the first member of a new epoxide hydrolase family with high activity for fatty acid epoxides. *J. Lipid Res.* **53**: 2038-2045.

15. Toulza, E., N. R. Mattiuzzo, M. F. Galliano, N. Jonca, C. Dossat, D. Jacob, A. de Daruvar, P. Wincker, G. Serre, and M. Guerrin. 2007. Large-scale identification of human genes implicated in epidermal barrier function. *Genome Biol.* **8**: R107.

16. Ala, U., R. M. Piro, E. Grassi, C. Damasco, L. Silengo, M. Oti, P. Provero, and F. Di Cunto. 2008. Prediction of human disease genes by human-mouse conserved coexpression analysis. *PLoS Comput. Biol.* **4**: e1000043.

17. Thomas, C. P., W. E. Boeglin, Y. Garcia-Diaz, V. B. O'Donnell, and A. R. Brash. 2013. Steric analysis of epoxyalcohol and trihydroxy derivatives of 9-hydroperoxy-linoleic acid from hematin and enzymatic synthesis. *Chem. Phys. Lipids* **167-168**: 21-32.

18. Gibson, T., and P. Strassburger. 1976. Sulfinic acid catalyzed isomerization of olefins. *J. Org. Chem.* **41**: 791-793.

19. Zheng, Y., W. E. Boeglin, C. Schneider, and A. R. Brash. 2008. A 49-kDa mini-lipoxygenase from Anabaena sp. PCC 7120 retains catalytically complete functionality. *J. Biol. Chem.* **283**: 5138-5147.

20. Tallman, K. A., B. Roschek, Jr., and N. A. Porter. 2004. Factors influencing the autoxidation of fatty acids: effect of olefin geometry of the nonconjugated diene. *J. Am. Chem. Soc.* **126**: 9240-9247.

21. Gao, B., W. E. Boeglin, Y. Zheng, C. Schneider, and A. R. Brash. 2009. Evidence for an ionic intermediate in the transformation of fatty acid hydroperoxide by a catalase-related allene oxide synthase from the Cyanobacterium Acaryochloris marina. *J. Biol. Chem.* **284**: 22087-22098.

22. Weyer, U., S. Knight, and R. D. Possee. 1990. Analysis of very late gene expression by Autographa californica nuclear polyhedrosis virus and the further development of multiple expression vectors. *J. Gen. Virol.* **71**: 1525-1534.

23. Beetham, J. K., T. G. Tian, and B. D. Hammock. 1993. cDNA Cloning and Expression of a Soluble Epoxide Hydrolase from Human Liver. *Arch. Biochem. Biophys.* **305**: 197-201.

24. Morisseau, C., J. W. Newman, C. E. Wheelock, T. Hill Iii, D. Morin, A. R. Buckpitt, and B. D. Hammock. 2008. Development of Metabolically Stable Inhibitors of Mammalian Microsomal Epoxide Hydrolase. *Chem. Res. Toxicol.* **21**: 951-957.

25. Wixtrom, R. N., M. H. Silva, and B. D. Hammock. 1988. Affinity purification of cytosolic epoxide hydrolase using derivatized epoxy-activated Sepharose gels. *Anal. Biochem.* **169**: 71-80.

26. Akatsuka, T., N. Kobayashi, T. Ishikawa, T. Saito, M. Shindo, M. Yamauchi, K. Kurokohchi, H. Miyazawa, H. Duan, T. Matsunaga, T. Komoda, C. Morisseau, and B. D. Hammock. 2007. Autoantibody response to microsomal epoxide hydrolase in hepatitis C and A. *J. Autoimmunity* **28**: 7-18.

27. Morisseau, C., and B. D. Hammock. 2001. Measurement of Soluble Epoxide Hydrolase (sEH) Activity. *In* Curr. Protoc. Toxicol. John Wiley & Sons, Inc.

28. Lambers, H., S. Piessens, A. Bloem, H. Pronk, and P. Finkel. 2006. Natural skin surface pH is on average below 5, which is beneficial for its resident flora. *Int. J. Cosmet. Sci.* **28**: 359-370.

29. Braun-Falco, O., and H. C. Korting. 1986. [Normal pH value of human skin]. *Der Hautarzt; Zeitschrift fur Dermatologie, Venerologie, und verwandte Gebiete* **37**: 126-129.

30. Jiang, H., A. G. Zhu, M. Mamczur, C. Morisseau, B. D. Hammock, J. R. Falck, and J. C. McGiff. 2008. Hydrolysis of cis- and trans-epoxyeicosatrienoic acids by rat red blood cells. *J. Pharmacol. Exp. Ther.* **326**: 330-337.

31. Moghaddam, M., D. F. Grant, J. M. Cheek, J. Greene, K. C. Williamson, and B. D. Hammock. 1997. Bioactivation of leukotoxins to their toxic diols by epoxide hydrolase.

32. Sinal, C. J., M. Miyata, M. Tohkin, K. Nagata, J. R. Bend, and F. J. Gonzalez. 2000. Targeted disruption of soluble epoxide hydrolase reveals a role in blood pressure regulation. *J. Biol. Chem.* **275**: 40504-40510.

33. Hoopes, S. L., A. Gruzdev, M. L. Edin, J. P. Graves, J. A. Bradbury, G. P. Flake, F. B. Lih, L. M. DeGraff, and D. C. Zeldin. 2017. Generation and characterization of epoxide hydrolase 3 (EPHX3)-deficient mice. *PloS one* **12**: e0175348.

34. Enayetallah, A. E., R. A. French, M. S. Thibodeau, and D. F. Grant. 2004. Distribution of soluble epoxide hydrolase and of cytochrome P450 2C8, 2C9, and 2J2 in human tissues. *J. Histochem. Cytochem.* **52**: 447-454.

35. Corey, E. J., H. Niwa, and J. R. Falck. 1979. Selective epoxidation of eicosa-cis-5,8,11,14-tetraenoic (arachidonic) acid and eicosa-cis-8,11,14-trienoic acid. *J. Am. Chem. Soc.* **101**: 1586-1587.

36. VanderNoot, V. A., and M. VanRollins. 2002. Capillary electrophoresis of cytochrome P-450 epoxygenase metabolites of arachidonic acid. 1. Resolution of regioisomers. *Anal. Chem.* **74**: 5859-5865.

37. Fitzpatrick, F. A., D. R. Morton, and M. A. Wynalda. 1982. Albumin stabilizes leukotriene A4. *J. Biol. Chem.* **257**: 4680-4683.

38. Hamberg, M. 1987. Mechanism of corn hydroperoxide isomerase: detection of 12,13(S)-oxido-9(Z),11-octadecadienoic acid. *Biochim. Biophys. Acta* **920**: 76-84.

39. Hamberg, M. 2000. New cyclopentenone fatty acids formed from linoleic and linolenic acids in potato. *Lipids* **35**: 353-363.

40. Pace-Asciak, C. R. 2015. Pathophysiology of the hepoxilins. *Biochim. Biophys. Acta* **1851**: 383-396.

41. Chawengsub, Y., K. M. Gauthier, K. Nithipatikom, B. D. Hammock, J. R. Falck, D. Narsimhaswamy, and W. B. Campbell. 2009. Identification of 13-hydroxy-14,15-epoxyeicosatrienoic acid as an acid-stable endothelium-derived hyperpolarizing factor in rabbit arteries. *J. Biol. Chem.* **284**: 31280-31290.

42. Krieg, P., S. Rosenberger, S. de Juanes, S. Latzko, J. Hou, A. Dick, U. Kloz, F. van der Hoeven, I. Hausser, I. Esposito, M. Rauh, and H. Schneider. 2013. Aloxe3 knockout mice reveal a function of epidermal lipoxygenase-3 as hepoxilin synthase and its pivotal role in barrier formation. *J. Invest. Dermatol.* **133**: 172-180.

43. Ohno, Y., S. Nakamichi, A. Ohkuni, N. Kamiyama, A. Naoe, H. Tsujimura, U. Yokose, K. Sugiura, J. Ishikawa, M. Akiyama, and A. Kihara. 2015. Essential role of the cytochrome P450 CYP4F22 in the production of acylceramide, the key lipid for skin permeability barrier formation. *Proc. Natl. Acad. Sci. USA* **112**: 7707-7712.

44. Hirabayashi, T., T. Anjo, A. Kaneko, Y. Senoo, A. Shibata, H. Takama, K. Yokoyama, Y. Nishito, T. Ono, C. Taya, K. Muramatsu, K. Fukami, A. Muñoz-Garcia, A. R. Brash, K. Ikeda, M. Arita, M. Akiyama, and M. Murakami. 2017. PNPLA1 has a crucial role in skin barrier function by directing acylceramide biosynthesis. *Nat. Commun.* **8**: 14609.

45. Grond, S., T. O. Eichmann, S. Dubrac, D. Kolb, M. Schmuth, J. Fischer, D. Crumrine, P. M. Elias, G. Haemmerle, R. Zechner, A. Lass, and F. P. W. Radner. 2017. PNPLA1 Deficiency in Mice and Humans Leads to a Defect in the Synthesis of Omega-O-Acylceramides. *J. Invest. Dermatol.* **137**: 394-402.

46. Grond, S., F. P. W. Radner, T. O. Eichmann, D. Kolb, G. F. Grabner, H. Wolinski, R. Gruber, P. Hofer, C. Heier, S. Schauer, T. Rülicke, G. Hoefler, M. Schmuth, P. M. Elias, A. Lass, R. Zechner, and G. Haemmerle. 2017. Skin Barrier Development Depends on CGI-58 Protein Expression during Late-Stage Keratinocyte Differentiation. *J. Invest. Dermatol.* **137**: 403-413.

47. Madison, K. C. 2003. Barrier Function of the Skin: “La Raison d'Être” of the Epidermis. *J. Invest. Dermatol.* **121**: 231-241.

48. Eckl, K. M., S. de Juanes, J. Kurtenbach, M. Natebus, J. Lugassy, V. Oji, H. Traupe, M. L. Preil, F. Martinez, J. Smolle, A. Harel, P. Krieg, E. Sprecher, and H. C. Hennies. 2009. Molecular analysis of 250 patients with autosomal recessive congenital ichthyosis: evidence for mutation hotspots in ALOXE3 and allelic heterogeneity in ALOX12B. *J. Invest. Dermatol.* **129**: 1421-1428.

49. Elias, P. M., and M. Schmuth. 2009. Abnormal skin barrier in the etiopathogenesis of atopic dermatitis. *Curr. Opin. Allergy Clin. Immunol.* **9**: 437-446.

50. Elias, P. M., and J. Wakefield. 2014. Mechanisms of abnormal lamellar body secretion and the dysfunctional skin barrier in atopic dermatitis. *J. Allergy Clin. Immunol.* **134**: 781-791.e781.

FIGURES

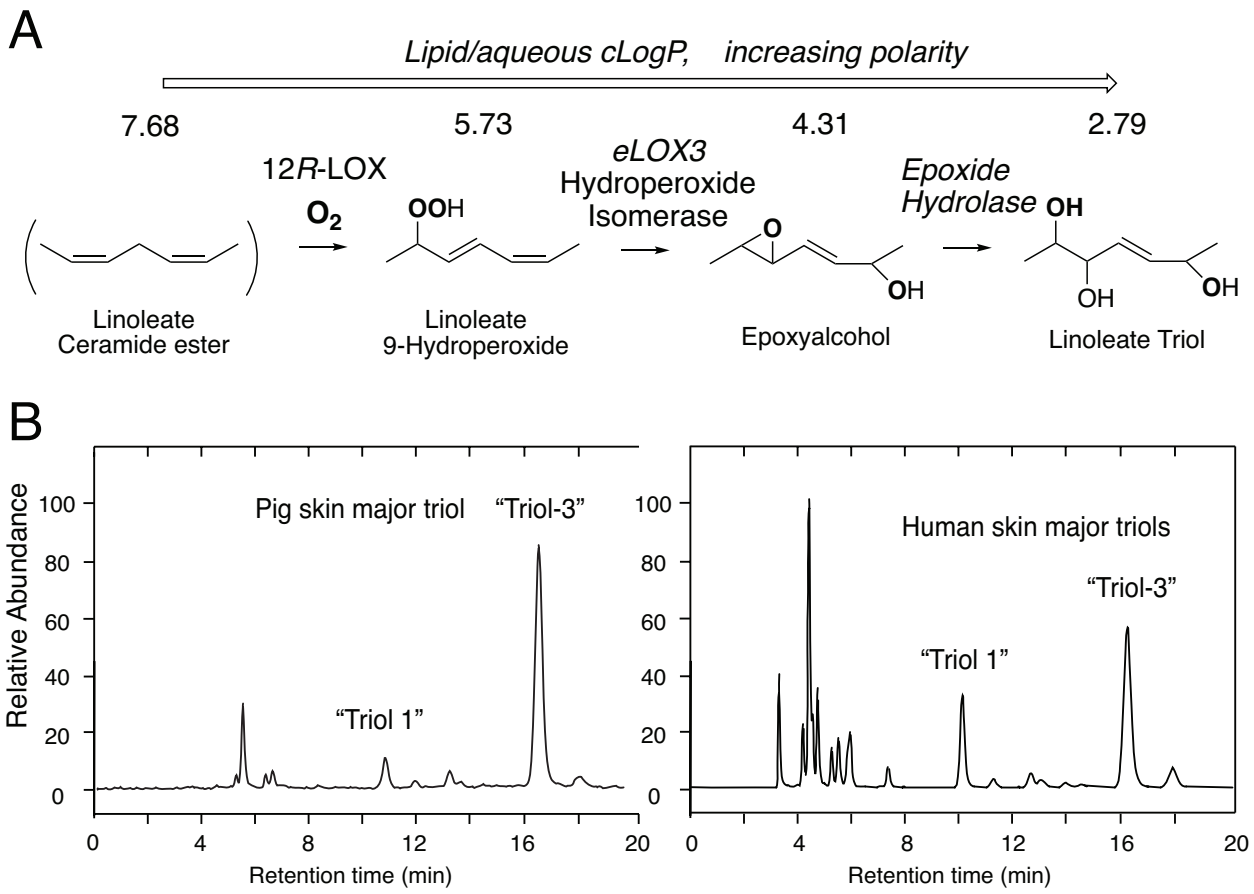

Figure 1. The proposed 12R-lipoxygenase pathway in the mammalian epidermis and formation of linoleate triols

A: The 12R-LOX/eLOX3 pathway of the mammalian epidermis and proposed involvement of epoxide hydrolase forming linoleate triol. The stepwise transformations increase the polarity of the unionized fatty acid moiety (indicated by the decreased lipid/aqueous partition coefficients, cLogP calculated by ChemDraw).

B: Previously reported patterns of linoleate triols esterified in Cer-EOS as detected by LC-MS of pig and human epidermis (7). Structures of Triol-1 and -3 are the same as illustrated later in Figures 5A of Results.

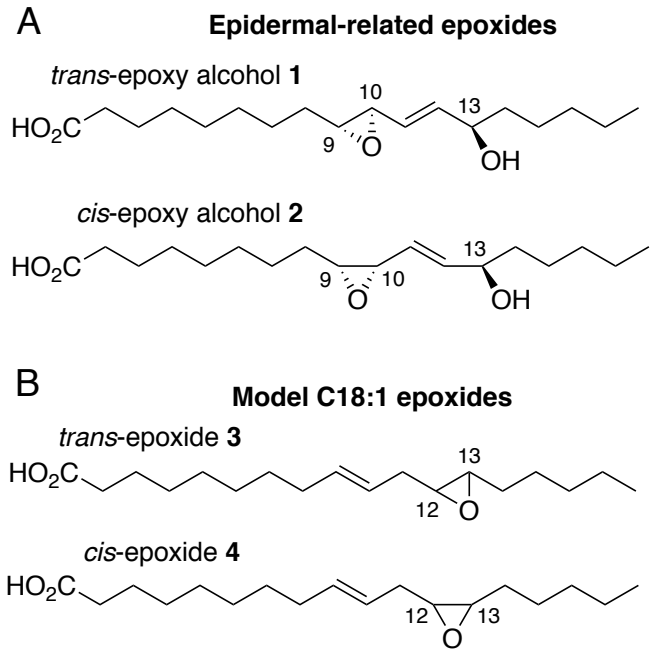

Figure 2. Structures of the linoleate-derived *trans* and *cis* allylic epoxyalcohols 1 and 2 and the model *cis* and *trans* fatty acid epoxides 3 and 4

The epidermal-related epoxides are *trans*-epoxyalcohol **1**, 9*R*,10*R*-*trans*-epoxy-13*R*-hydroxy-octadec-11*E*-enoic acid, and *cis*-epoxyalcohol **2**, 9*R*,10*S*-*cis*-epoxy-13*R*-hydroxy-octadec-11*E*-enoic acid. The model C18:1 epoxides are 12,13-*trans*-epoxy-octadeca-9*E*-enoic acid (**3**), and 12,13-*cis*-epoxy-octadeca-9*E*-enoic acid (**4**).

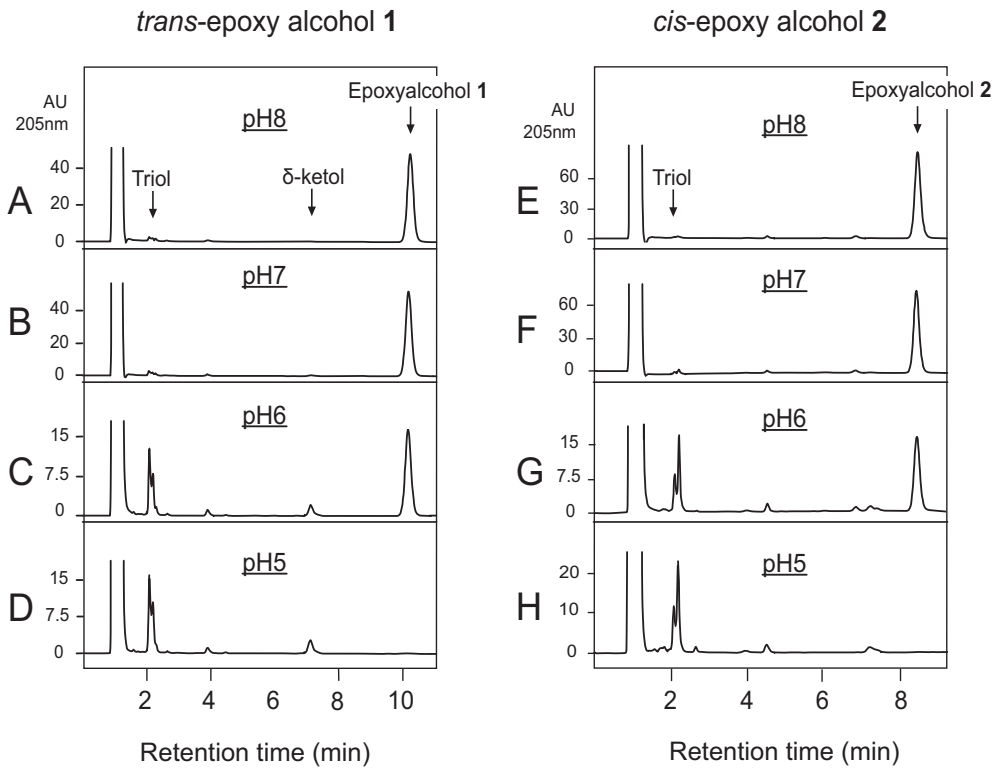

Figure 3. RP-HPLC analysis of the pH sensitivity of epoxyalcohols 1 and 2 exposed to pH 5 – 8

trans-Epoxyalcohol **1** and *cis*-epoxyalcohol **2** (30 μM) were incubated in 50 μl aliquots of 0.1 M phosphate buffers at pH, 5, 6, 7, or 8 for 30 min/1 h at 37°C. The samples were then injected directly on RP-HPLC. The HPLC analysis used a Kinetex 2.6 μ 100 x 3 mm column with an isocratic solvent acetonitrile/water/glacial acetic acid (45/55/0.01, by volume) at a flow rate of 0.4 ml/min with UV detection at 205 nm. Retention times are illustrated for the starting material (epoxyalcohol), and the triol hydrolysis products and a δ-ketol formed during acid-catalyzed rearrangement (17).

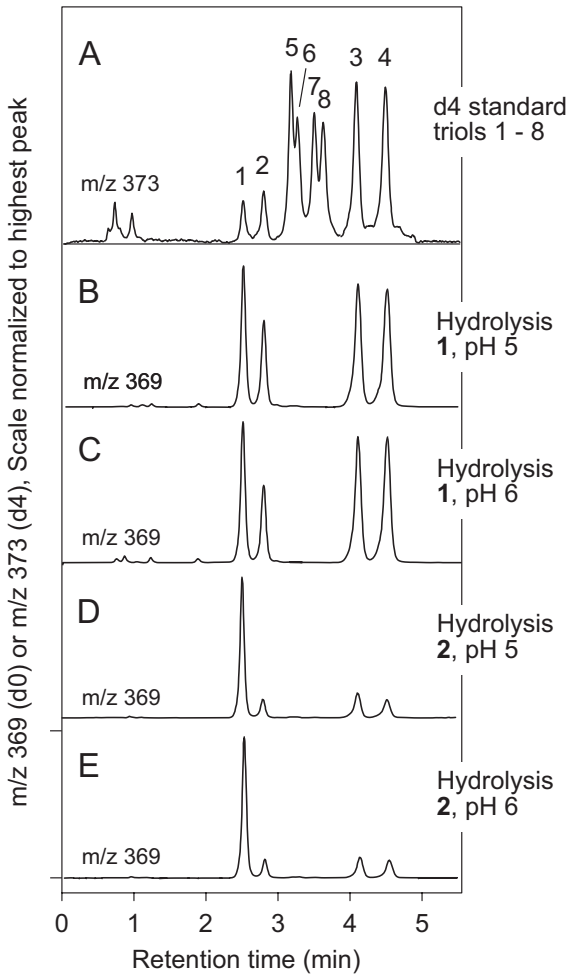

Figure 4. Identification of the triol products of non-enzymatic hydrolysis of epoxyalcohols 1 and 2

Triol isomers were separated on LC-MS by SP-HPLC of the 1,2-acetonide PFB ester derivative and detected as the M – PFB ion at m/z 369(7). Panel A, the top chromatogram illustrates separation of eight triol isomers; panels B and C show that *trans*-epoxyalcohol **1** is hydrolyzed at pH 5 or pH 6 to a mixture of triols 1, 2, 3 and 4. Panels D and E: the *cis*-epoxyalcohol **2** is hydrolyzed at pH 5 or pH 6 to a mixture of four triols, predominantly 1, and also including triols 2, 3, and 4. The HPLC analysis used a Phenomenex Hilic column (100 x 2 mm) with a solvent system of hexane/IPA (100:1 v/v/) at a flow rate of 0.5 ml/min.

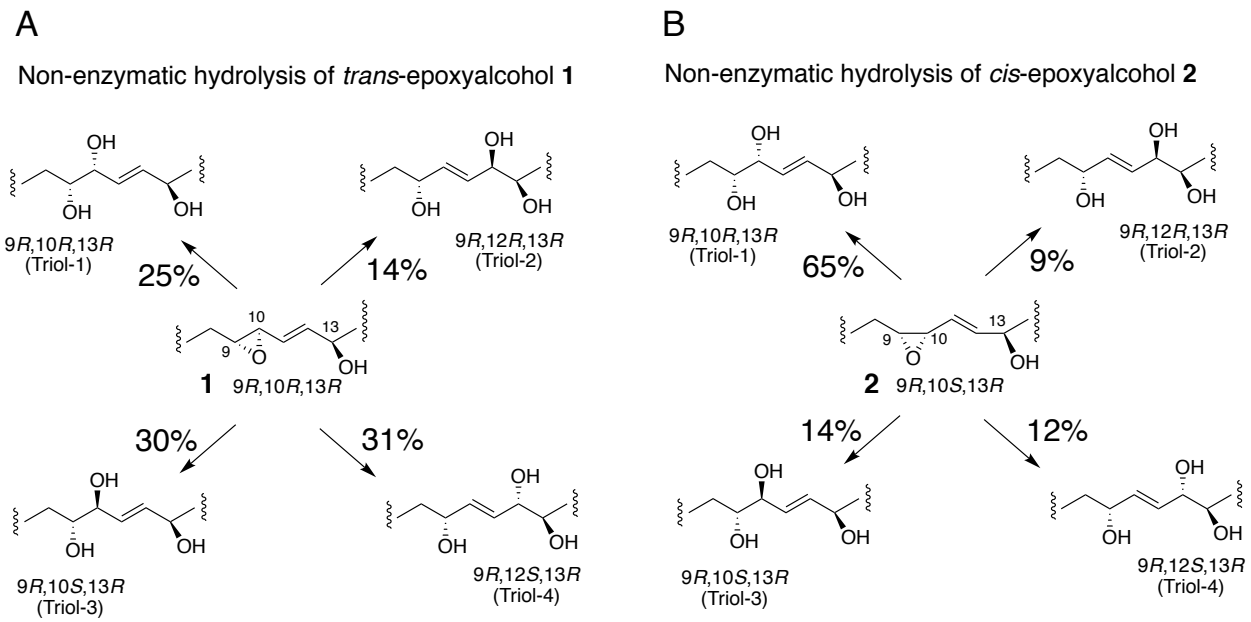

Figure 5. Structures of the triol products of non-enzymatic hydrolysis of epoxyalcohols 1 and 2

The percentage of each triol product of non-enzymatic hydrolysis is shown next to the arrows.

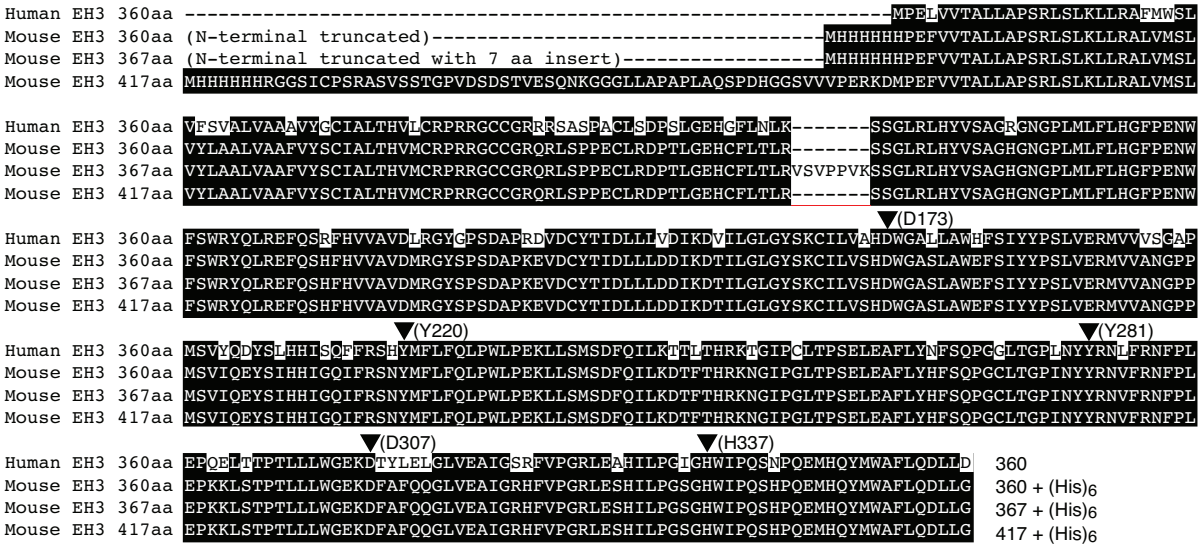

Figure 6. Amino acid sequences of epoxide hydrolase 3 (EH3, EPHX3).

On top is the sequence of human EH3. Below are three constructs of mouse EH3 prepared for testing in the current study, each with a N-terminal $(His)_6$ tag: (i) truncated mouse EH3 with the rodent-specific 57 amino acid N-terminus removed, (ii) truncated mouse EH3 containing a 7-amino acid insert (VSVPPVK) at position 138, and (iii) full-length mouse EH3. Arrowheads (with numbering of human EH3 residues) indicate the α/β-hydrolase catalytic triad (D173, D307, H337) and the two tyrosines (Y220, Y281) important for initial activation of the oxiran ring (14).

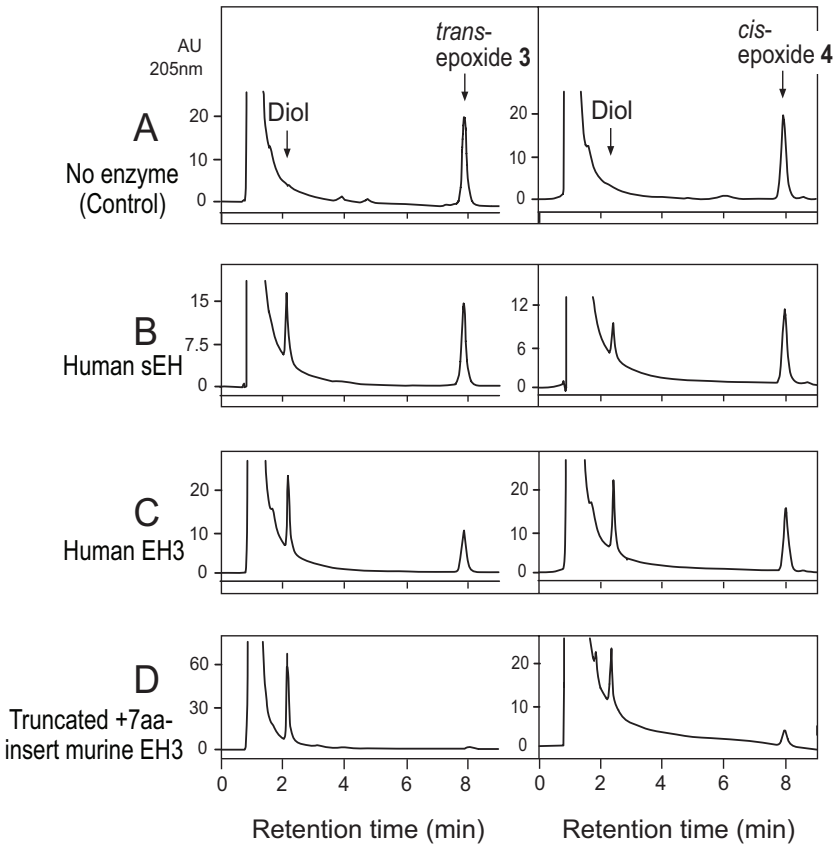

Figure 7. Comparison of the enzymatic hydrolysis of model *cis* and *trans* fatty acid epoxides 3 and 4

The *trans*-epoxide **3** and the *cis*-epoxide **4** were incubated in 50 µl aliquots of 0.1 M phosphate buffers at pH 8 with human sEH, human EH3, and truncated mouse EH3 containing the 7-amino acid insert (cf. Fig 6). The samples were then injected directly on RP-HPLC; the samples were slightly acidified by addition of 2 µl of 10-fold dilute glacial acetic acid immediately before injection on column. The HPLC analysis used a Kinetex 2.6 µ 100 x 3 mm column with an isocratic solvent acetonitrile/water/glacial acetic acid (60/40/0.01, by volume) at a flow rate of 0.4 ml/min with UV detection at 205 nm. Retention times are illustrated for the starting material (model fatty acid epoxide) and the diol hydrolysis products.

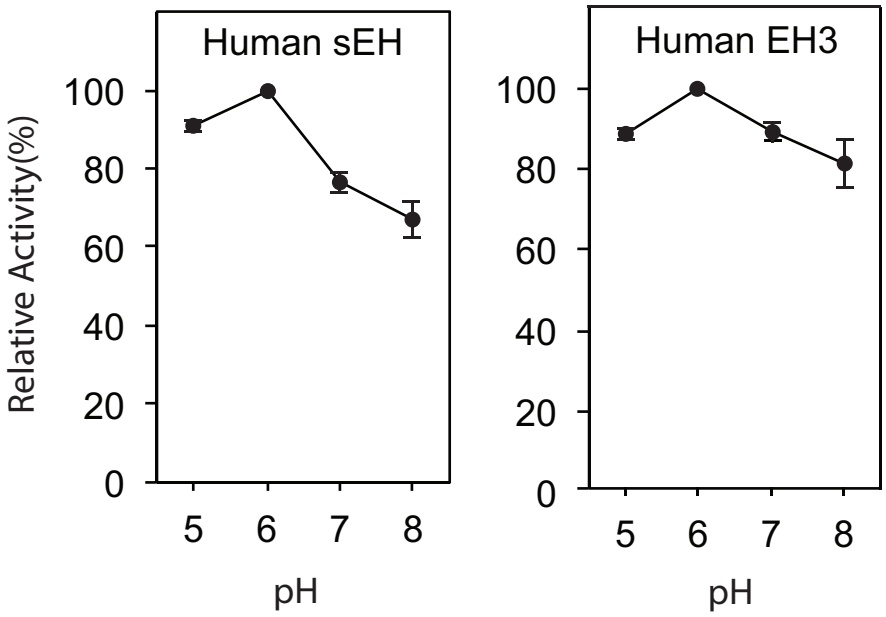

Figure 8. pH profile of epoxide hydrolase activities with *trans-epoxide 3*

The model *trans*-epoxide **3** (50 μM) was incubated in 50 μl aliquots of 0.1 M phosphate buffers at pH, 5, 6, 7, or 8 for 30 min at 37°C with human sEH and human EH3. The samples were then injected directly on RP-HPLC; the pH 7 and 8 samples were slightly acidified before injection on column. Chromatographic conditions were the same as in Figure 7. The data points represent n = 3, +/- range.

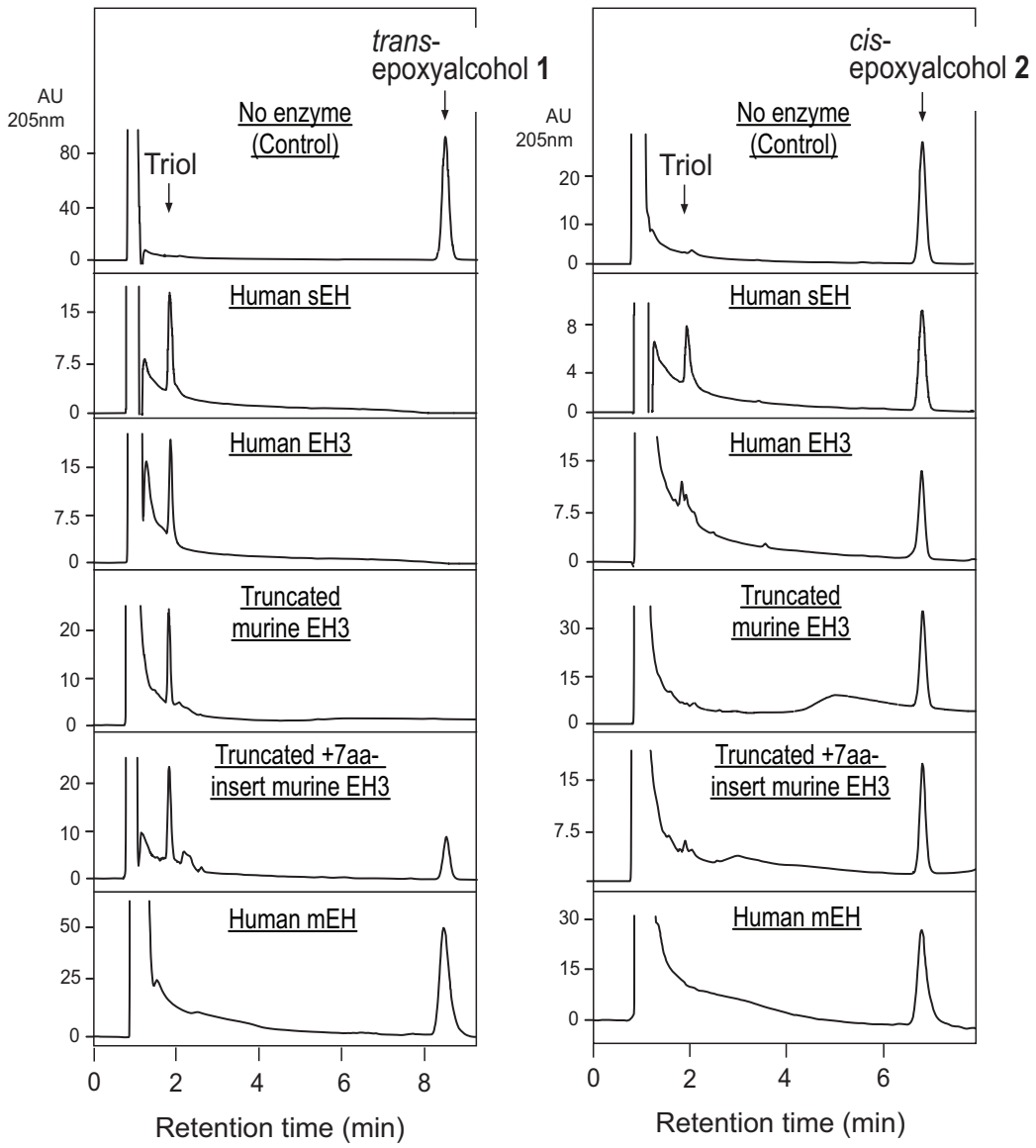

Figure 9. RP-HPLC analysis of the hydrolysis of epoxyalcohols 1 and 2 by epoxide hydrolases

The *trans*-epoxyalcohol **1** and the *cis*-epoxyalcohol **2** were incubated in 50 µl aliquots of Tris buffer (10 mM, pH 8.0) with human sEH, human EH3, two N-terminally truncated constructs of mouse EH3 (with and without the 7 amino acid insert, Fig 6), and human mEH. Chromatographic conditions were the same as in Fig 3. Retention times are illustrated for the starting material (epoxyalcohol) and the triol hydrolysis products.

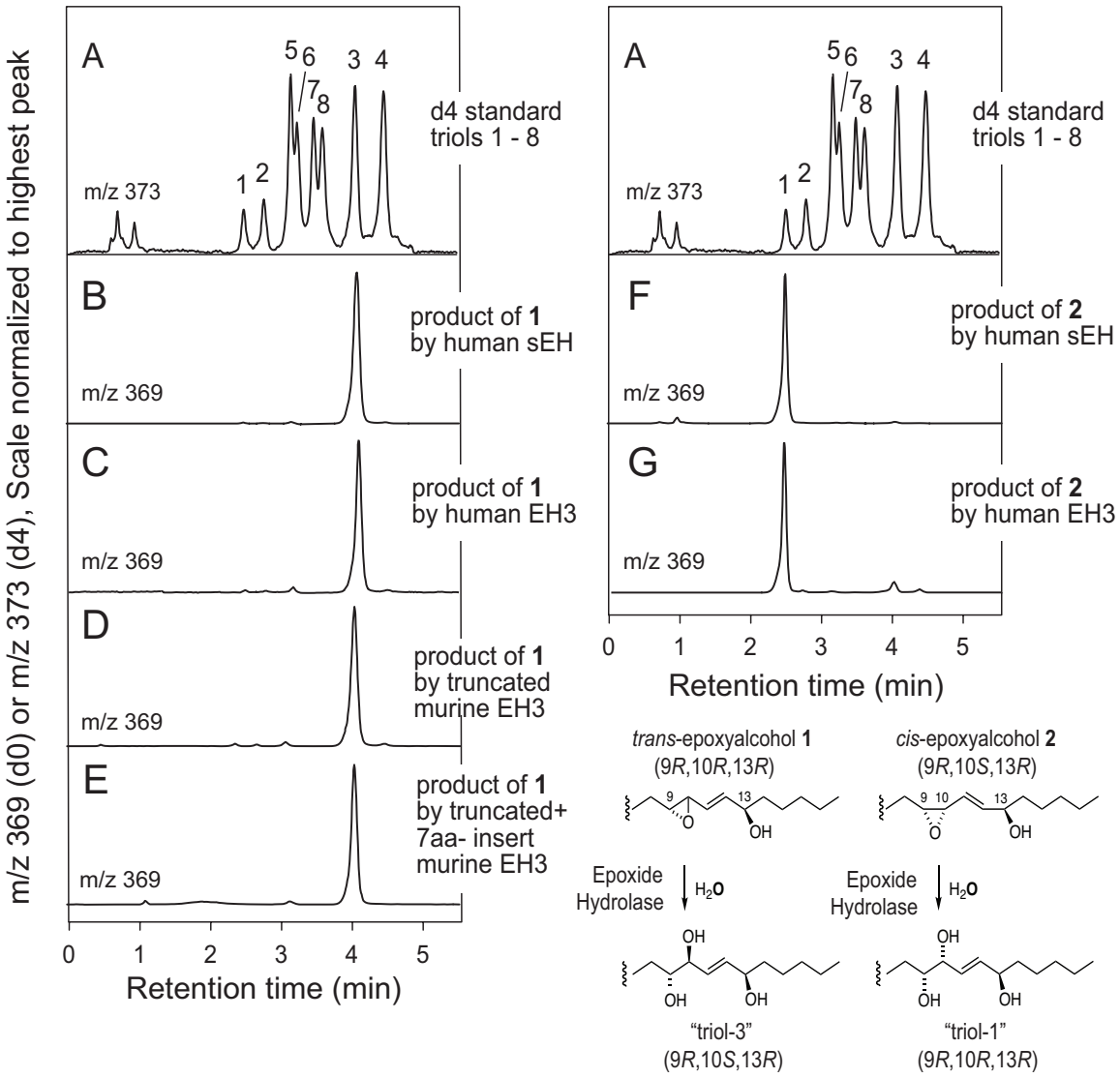

Figure 10. Identification of the triol products of enzymatic hydrolysis of epoxyalcohols 1 and 2

Triol isomers were separated on LC-MS by SP-HPLC of the 1,2-acetonide PFB ester derivative and detected as the M – PFB ion at m/z 369 (7). Left-hand side: panel A, the top chromatogram illustrates separation of eight triol isomers; panels B, C, D, and E show that human sEH, human EH3 and two constructs of mouse EH3 each hydrolyze epoxyalcohol **1** exclusively to triol 3. Right-hand side: panel F and G show that human sEH and human EH3 hydrolyze epoxyalcohol **2** exclusively to triol 1. The HPLC analysis used a Phenomenex Hilic column (100 x 2 mm) with a solvent system of hexane/IPA (100:1 v/v/) at a flow rate of 0.4 ml/min.

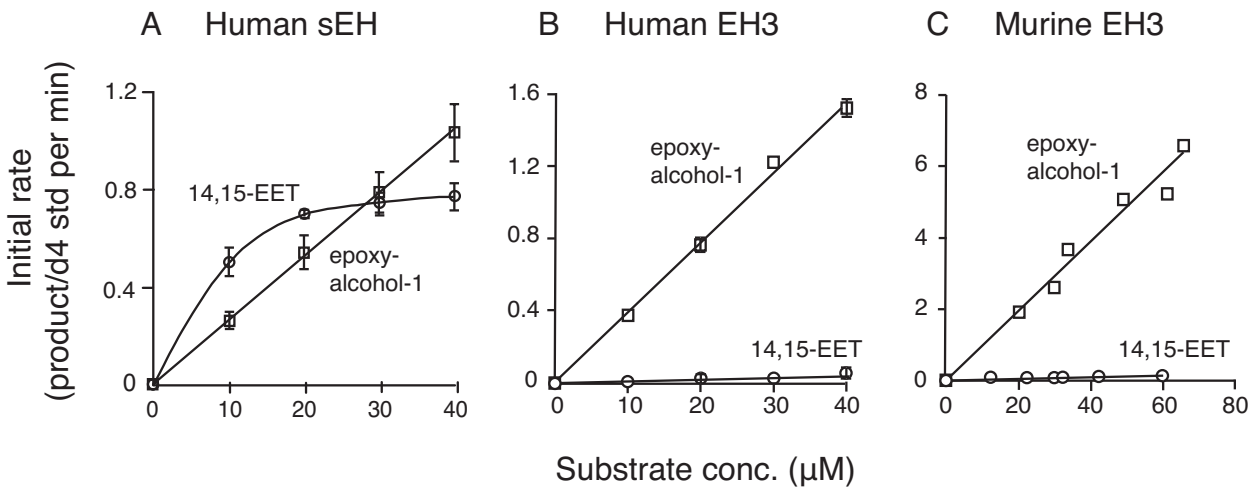

Figure 11. Comparison of the rates of hydrolysis of *trans*-epoxyalcohol 1 and 14,15-EET

The initial rates of transformation of *trans*-epoxyalcohol **1** (□) and 14,15-EET (○) are plotted against concentration of the epoxide on incubation with (A) human sEH, (B) human EH3, and (C) truncated mouse EH3. Incubations were conducted in 50 μl aliquots of 0.1 M phosphate buffer at pH 8 at 37 °C and terminated by addition of 50 μl acetonitrile and deuterated internal standards (d4-triol or d8-diol). The samples were analyzed using a Kinetex 2.6 μ C18 column (100 x 3 mm) with an isocratic solvent of acetonitrile/15mM ammonium acetate pH 8.5 (25/75, by volume for triol analysis and 35/65, by volume for diol) at a flow rate of 0.4 ml/min, with LC-MS detection at m/z 329 (do) and 333 (d4) for the triol product from *trans*-epoxyalcohol **1** and m/z 337 (do) and 345 (d8) for the diol product from 14.15-EET. The graph was obtained by using KaleidaGraph 4.0 (Synergy Software, Reading, PA); for panels A and B, n = 4, mean ± S.E.M; for panel C, data points represent the average of two or three determinations from two independent experiments).